Neuron, Vol. 36, 933–944, December 5, 2002, Copyright ©2002 by Cell Press

Decoding of Polymodal Sensory Stimuli by Postsynaptic Glutamate Receptors in *C. elegans*

Jerry E. Mellem,[2] Penelope J. Brockie,[2] Yi Zheng, David M. Madsen, and Andres V. Maricq[1]
Department of Biology
University of Utah
Salt Lake City, Utah 84112

Summary

The *C. elegans* polymodal ASH sensory neurons detect mechanical, osmotic, and chemical stimuli and release glutamate to signal avoidance responses. To investigate the mechanisms of this polymodal signaling, we have characterized the role of postsynaptic glutamate receptors in mediating the response to these distinct stimuli. By studying the behavioral and electrophysiological properties of worms defective for non-NMDA (GLR-1 and GLR-2) and NMDA (NMR-1) receptor subunits, we show that while the osmotic avoidance response requires both NMDA and non-NMDA receptors, the response to mechanical stimuli only requires non-NMDA receptors. Furthermore, analysis of the EGL-3 proprotein convertase provides additional evidence that polymodal signaling in *C. elegans* occurs via the differential activation of postsynaptic glutamate receptor subtypes.

Introduction

Elucidating the mechanisms whereby distinct sensory stimuli detected by a specific class of sensory neurons are distinguished by the nervous system has been a major challenge for neurobiology. For example, nociceptive sensory neurons are typically polymodal and transduce a variety of aversive stimuli such as heat, pressure, and chemicals into signals that are perceived as pain (Julius and Basbaum, 2001). These stimuli can be distinguished as different types of pain sensations, implying that polymodal signals received by nociceptive sensory neurons are somehow decoded by the nervous system into distinct classes of pain (Woolf and Salter, 2000).

In *C. elegans*, the bilateral pair of ASH polymodal sensory neurons respond to tactile stimuli, osmotic strength, and aversive chemicals. In all cases, the ASH neurons signal to the worm to withdraw from the stimulus and in this regard may be thought of as transmitting nociceptive stimuli (Kaplan and Horvitz, 1993; Bargmann and Kaplan, 1998). The neural circuit for this withdrawal response is reasonably well understood. Of primary importance are five pairs of interneurons that process inputs from ASH sensory neurons–AVA, AVB, AVD, AVE, and PVC (Chalfie et al., 1985; White et al., 1986; Zheng et al., 1999). Screening for genetic mutations that disrupt avoidance behavior has identified molecules that contribute to ASH signaling. These gene products include the OSM-9 protein, which is likely to form part of a channel complex that is required for transduction of both osmotic and mechanical stimuli (Colbert et al., 1997); the OSM-10 protein, which is required for the detection of osmotic stimuli, but not tactile stimuli (Hart et al., 1999); and the EAT-4 vesicular glutamate transporter (Lee et al., 1999; Bellocchio et al., 2000; Takamori et al., 2000). EAT-4 is required for avoidance of all the sensory stimuli detected by ASH, suggesting that glutamate is the neurotransmitter released by the ASH neurons (Berger et al., 1998).

The general question of how polymodal sensory information is decoded has been difficult to address. One insight was provided in *C. elegans* by the observation that mutations in the *glr-1* gene were found to selectively disrupt the withdrawal response to specific tactile stimuli, but not to osmotic stimuli (Hart et al., 1995; Maricq et al., 1995). *glr-1* encodes an ionotropic glutamate receptor subunit that is expressed postsynaptically in the interneuron targets of the ASH neurons. This observation suggested that mechanical and osmotic stimuli may be mediated by distinct neurotransmitters, may activate different subsets of glutamate receptors, or may reflect differential release of glutamate and/or a peptide cotransmitter. We have previously shown that at least ten glutamate receptor subunits are expressed in the nervous system of *C. elegans* (Brockie et al., 2001a). Of these, *glr-2* encodes a subunit with the highest identity to GLR-1. Furthermore, GLR-1 and GLR-2 are coexpressed in a number of neurons that include the central interneurons of the locomotory control circuit (AVA, AVD, AVE, and PVC) (Brockie et al., 2001a). Thus, GLR-2 may function either together or independently of GLR-1 to mediate avoidance responses dependent on ASH. We therefore hypothesized that mutations in both *glr-1* and *glr-2* may affect the response to osmotic as well as tactile stimuli.

Recently, it has been shown that mutations in the *egl-3* gene suppress the mechanosensory defects of *glr-1* mutants (Kass et al., 2001). *egl-3* encodes an ortholog of the PC2 family of proprotein convertases that process proneuropeptides into active signaling molecules. Neuropeptides have been shown to modulate pre- and postsynaptic function by altering neurotransmitter release from presynaptic neurons (Akopian et al., 2000; Silva et al., 2001) or by downregulating postsynaptic neurotransmitter receptors (Gao and van den Pol, 2001). Thus, *egl-3* may affect glutamatergic signaling in *C. elegans* by modulating pre- or postsynaptic function.

Here, we assess the contributions of individual glutamate receptor subunits to ASH-dependent avoidance behaviors. We show that the non-NMDA receptor subunits GLR-1 and GLR-2 function together with the NMDA subunit NMR-1 to mediate osmotic avoidance behavior. Furthermore, we show that a mutation in *egl-3* that suppresses the mechanosensory defects of *glr-1* mutants (Kass et al., 2001) also restored the osmotic avoidance response in these worms. Interestingly, the restoration of both behaviors was completely dependent on the NMR-1 subunit. Collectively, our findings suggest that

[1]Correspondence: maricq@biology.utah.edu
[2]These authors contributed equally to this work.

mechanical stimuli cause synaptic activation of non-NMDA-dependent currents, that osmotic signals activate both non-NMDA- and NMDA-dependent currents, and that EGL-3 modifies glutamate levels at ASH-interneuron synapses.

Results

glr-2 Encodes an Ionotropic Glutamate Receptor Subunit

To investigate the contribution of *glr-2* to polymodal signaling by ASH, we cloned the *glr-2* gene and show that it encodes a predicted protein of 977 amino acids. GLR-2 contains all of the signature features of ionotropic glutamate receptors, including the pore-forming region consisting of TMI, TMIII, and the selectivity filter TMII; the two ligand binding domains S1 and S2; and the highly conserved SYTANLAAF amino acid sequence in TMIII (Figure 1A). GLR-2 has highest sequence identity (43%) with the previously described non-NMDA subunit GLR-1 (Maricq et al., 1995; Brockie et al., 2001a). Interestingly, GLR-2 has a nonaromatic residue, glutamine (Q), at position 580 (position 507 in rat GluR3), which lies in a conserved ligand binding region in S1. At this position, vertebrate AMPA receptor subtypes have a nonaromatic residue, whereas an aromatic residue is found at this position in kainate receptors. Changing the amino acid residue at this site has dramatic effects on the rate of receptor desensitization following ligand binding (Stern-Bach et al., 1998).

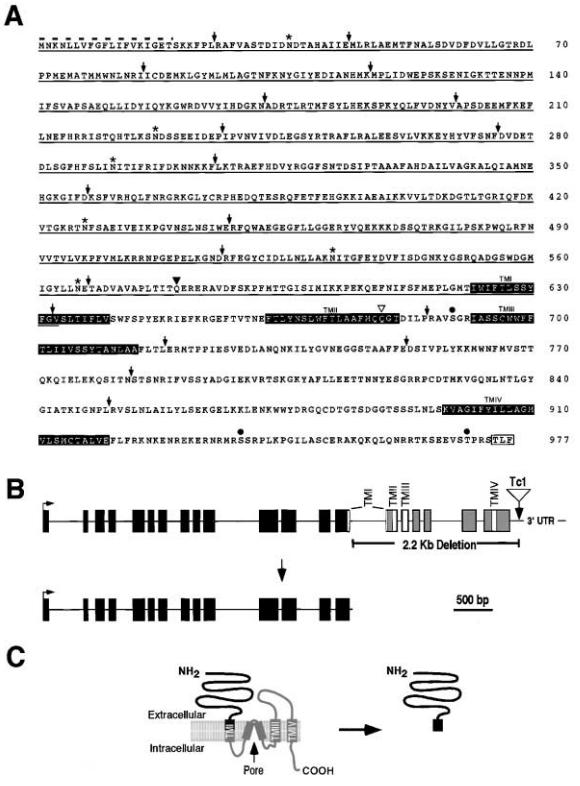

Figure 1. *glr-2* Encodes an Ionotropic Glutamate Receptor Subunit that Is Dramatically Truncated by the *ak10* Deletion Mutation

(A) The amino acid sequence of GLR-2. The predicted signal sequence is shown by the dotted bar. Arrows indicate the sites where introns are spliced from the immature transcript. Predicted *N*-linked glycosylation sites and protein kinase C phosphorylation sites are labeled with an asterisk or closed circle, respectively. The underlined region represents the truncated peptide encoded by the *glr-2(ak10)* deletion allele. Predicted hydrophobic domains are highlighted by black boxes. The white box indicates the type I PDZ domain binding motif. The closed triangle highlights the glutamine (Q) residue important for receptor desensitization, and the open triangle labels the Q/R site. (B) Genomic organization of the wild-type *glr-2* (top) and the mutant *glr-2(ak10)* (bottom). Exons are represented by boxes and introns by the lines between the boxes. Gray boxes and lines indicate exons and introns deleted by the *ak10* mutation, respectively. White boxes show domains predicted to encode the four hydrophobic domains. The arrow indicates the site of Tc1 insertion. (C) Predicted membrane topology of GLR-2 (left) and the truncated peptide encoded by the *ak10* allele (right).

glr-2(ak10) Mutants Are Defective in Mechanosensory Signaling

GLR-2 is coexpressed with GLR-1 in four of the five pairs of interneurons of the locomotory control circuit that regulates worm movement (AVA, AVD, AVE, and PVC) (Brockie et al., 2001a). A subset of these interneurons receives direct synaptic input from the ASH sensory neurons. To examine the role of GLR-2 in sensory signaling, we generated a deletion mutation in *glr-2* by first isolating a strain that contained the Tc1 transposon inserted just 3′ of the *glr-2* stop codon (Figure 1B). We then identified a chromosomal deletion caused by imprecise excision of Tc1, generating the deletion mutation *glr-2(ak10)*. The deletion removes 2.2 kb of DNA, and the truncated gene is predicted to encode a protein that is lacking the terminal 344 amino acids, including those believed to contribute to the pore forming and ligand binding regions of the protein (Figure 1C).

glr-2(ak10) mutants were indistinguishable from wild-type worms on the basis of gross movement and appearance. However, they often failed to initiate a backing escape response when lightly touched on the nose (*N*ose *t*ouch, Not, phenotype; Figure 2A) (Kaplan and Horvitz, 1993). The magnitude of this mechanosensory defect was less severe than that observed in *glr-1* mutants, and the defect in *glr-2(ak10) glr-1(ky176)* double mutants was similar to that observed in *glr-1(ky176)* mutants. The Not phenotype was rescued in transgenic *glr-2(ak10)* mutants that expressed the wild-type *glr-2* gene. Our results suggest that GLR-1 and GLR-2 contribute to a heteromeric receptor that mediates a synaptic current required for transmission of mechanosensory signaling from the ASH neurons. Worms with a mutation in *nmr-1* that encodes an NMDA receptor subunit showed a normal response to the nose touch stimulus (Figure 2A) (Brockie et al., 2001b).

To determine whether mutant worms were able to respond to osmotic stimuli, we performed a standard assay to test for osmotic avoidance (Culotti and Russell, 1978) and determined the percentage of worms that were able to escape from a ring of high osmotic solution within 20 min (Figure 2B). Interestingly, both *glr-2* and *glr-2 glr-1* mutants were indistinguishable from wild-type worms in this osmotic avoidance assay. Furthermore, the triple mutant, *nmr-1; glr-2 glr-1* was also indistinguishable from wild-type. These results were somewhat surprising given that loss-of-function mutations in *eat-4*,

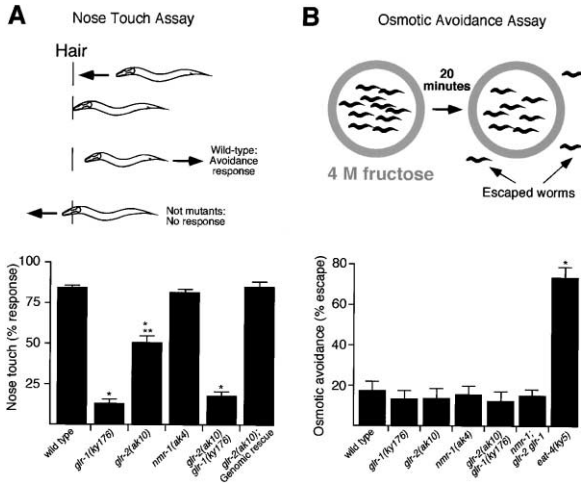

Figure 2. *glr-2(ak10)* Mutants Are Nose Touch Defective

(A) The nose touch assay (top). The worm's head is to the left and the arrows indicate the direction of movement. (Bottom) The percentage response to ten consecutive nose touch trials for wild-type worms (n = 44); the *glr-1* (n = 15), *glr-2* (n = 39), and *nmr-1* (n = 15) mutants; and the *glr-2 glr-1* double mutant (n = 15). *glr-2(ak10)*; genomic rescue (n = 15) were transgenic *glr-2* mutants that expressed a wild-type *glr-2* genomic clone. (B) The osmotic avoidance ring assay (top). (Bottom) The percentage of worms that escaped the osmotic barrier. The *glr-1* (n = 8), *glr-2* (n = 8), and *nmr-1* (n = 10) mutants and the double (n = 8) or triple (n = 8) mutants showed no defect, whereas *eat-4* mutants (n = 8) were defective for osmotic avoidance in the ring assay. *Statistical difference from wild-type ($p < 0.01$). **Statistical difference from wild-type and *glr-1(ky176)* ($p < 0.01$).

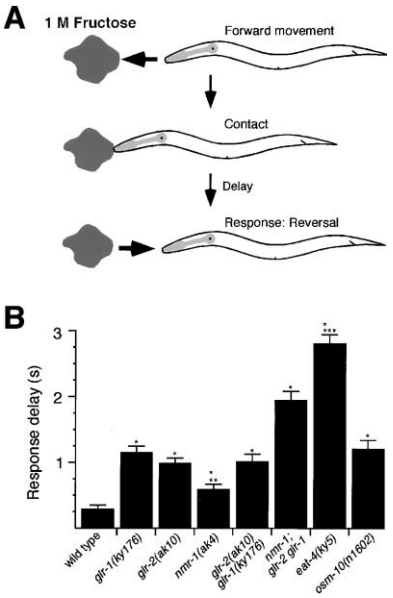

Figure 3. Mutations in *glr-1*, *glr-2*, and *nmr-1* Result in Osmotic Avoidance Defects

(A) The osmotic avoidance assay. Horizontal arrows indicate the direction of movement. (B) The average time taken (response delay) for a worm to reverse direction after contacting the fructose. Wild-type (n = 85), *glr-1* (n = 59), *glr-2* (n = 59), *nmr-1* (n = 57), *glr-2 glr-1* double mutant (n = 59), *nmr-1; glr-2 glr-1* triple mutant (n = 62), *eat-4* (n = 39), and *osm-10* (n = 57). Statistical difference from wild-type (*), *glr-1(ky176)* (**), or the *nmr-1; glr-2 glr-1* triple mutant (***); ($p < 0.01$). Given that the delay analysis requires that the worms respond to the stimulus, only worms that responded to the fructose were included in the analysis. A total of 61 *eat-4* mutants were screened, 22 of which did not respond to the stimulus. 1 in 60 *glr-1* mutants, 2 in 59 *nmr-1* mutants, 1 in 60 *glr-2 glr-1* double mutants, and 3 in 65 *nmr-1; glr-2 glr-1* triple mutants did not respond. 100% of the wild-type worms, and *glr-2* and *osm-10* mutants screened responded to the fructose.

which encodes a vesicular glutamate transporter, produce defects in both osmotic avoidance (Figure 2B) and the nose touch response (Berger et al., 1998). We hypothesized that these contrasting results may reflect assay conditions. Since the ring assay does not measure the immediate avoidance response to an osmotic stimulus and may reflect a variety of signaling processes including desensitization and adaptation, we used a new assay developed by Hilliard et al. (2002) that more directly examines osmotic avoidance behavior (see Experimental Procedures).

Glutamate Receptor Mutants Are Defective in Osmotic Avoidance

In the Hilliard assay, a small drop of control buffer or buffer with 1 M fructose (osmotic repellent) was placed in the path of a worm as it moved forward on an agar plate (Figure 3A). Wild-type and mutant worms that encountered the control buffer moved through the drop with no change in velocity or direction of movement (data not shown). In contrast, worms that encountered the fructose drop stopped their movement and initiated, after a brief delay, a backing response (Figure 3B). It is possible that this avoidance behavior reflects a mechanosensory response to contact with the solution. However, this is unlikely given that (1) wild-type worms do not respond to the control buffer, (2) worms that encounter the osmotic stimulus after the solution has been absorbed by the agar show an avoidance response comparable to worms that contact the solution on the agar surface, and (3) *osm-10* mutants that have defects in osmotic avoidance but show a normal response to mechanical stimuli are defective in the Hilliard assay (Hilliard et al., 2002) (Figure 3B).

Compared to wild-type worms, the delay in the withdrawal response was significantly increased in worms with mutations in glutamate receptor subunits. On average, wild-type worms took ~0.3 s to respond to the stimulus after the initial contact. In contrast, *glr-1* and *glr-2* mutants took ~1 s to respond and *nmr-1* mutants took about ~0.6 s. The delay observed in the *glr-2 glr-1* double mutant was no greater than for either single mutant alone. Interestingly, the delay in response observed in the *nmr-1; glr-2 glr-1* triple mutant (1.9 s) was greater than that in any of the single or double mutants ($p < 0.01$) and was approximately additive of the delay in the *nmr-1* mutant and the *glr-2 glr-1* double mutant. Compared to wild-type, the mutants showed no other obvious changes in locomotion. Our results show that both non-NMDA and NMDA receptors are activated by osmotic stimuli. Interestingly, the delay in the response observed in the triple mutant was not quite as severe as that observed in *eat-4* mutants ($p < 0.01$). These data indicate that the osmotic avoidance response may

recruit other glutamate receptor subunits to elicit a full response (Brockie et al., 2001a). Our data suggest that polymodal signaling at ASH-interneuron synapses occurs via stimulus-dependent activation of either non-NMDA receptors (nose touch response) or both non-NMDA and NMDA receptors (osmotic avoidance).

GLR-2 and GLR-1 Are Colocalized to Puncta in Neural Processes

The similar behavioral defects in the *glr-1* and *glr-2* mutants suggest that GLR-1 and GLR-2 are components of a functional glutamate-gated receptor. To determine the subcellular distribution of GLR-2, we generated transgenic strains that expressed a reporter construct in which green fluorescent protein (GFP) was fused in frame with full-length GLR-2 (GFP::GLR-2). In confirmation of our previous results (Brockie et al., 2001a), GFP expression was detected exclusively in neurons and was observed in both the cell bodies and processes. In the processes of the nerve ring and ventral cord (Figure 4A), expression was punctate in appearance, suggesting that GFP::GLR-2 was localized to synaptic regions (Rongo et al., 1998). To determine whether GLR-1 and GLR-2 localize to the same puncta, we generated transgenic strains that expressed GLR-1 fused to a cyan variant of GFP (GLR-1::CFP) and GLR-2 fused to a yellow variant of GFP (GLR-2::YFP). Using confocal microscopy, we detected colocalization of GLR-1::CFP and GLR-2::YFP in the cell body and neural processes (Figures 4B1–4B3). We determined that at specific puncta in the ventral cord processes, the CFP and YFP signals overlapped, indicating that these receptors colocalized and therefore may form heteromeric receptor complexes (Figures 4C1–4C3). In some instances, the GLR-1::CFP and GLR-2::YFP puncta did not colocalize. This was expected given that some cells that express GLR-1 do not express GLR-2 (Brockie et al., 2001a).

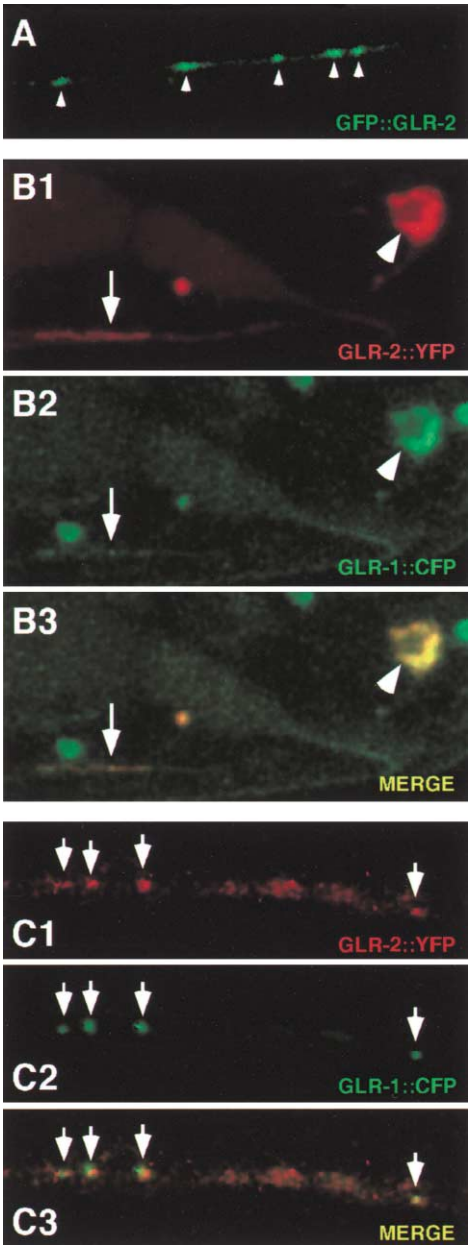

Figure 4. GLR-1::CFP and GLR-2::YFP Colocalize in Neuronal Cell Bodies and at Puncta in Neuronal Processes

(A) A confocal image of the ventral cord from a transgenic worm that expressed GFP::GLR-2. Puncta along the processes suggests that the fusion protein was localized to postsynaptic sites (arrowheads). (B1–B3) Confocal images of a transgenic worm that expressed GLR-2::YFP (B1) and GLR-1::CFP (B2). Expression was observed in the cell body of the PVC neuron (arrowhead) and in the neuronal processes (arrow). Colocalization of GLR-2::YFP and GLR-1::CFP in both the cell body and neuronal processes was evident in the merged image (B3). (C1–C3) Confocal images of the ventral cord of a transgenic worm that expressed GLR-2::YFP (C1) and GLR-1::CFP (C2). The GLR-2::YFP and GLR-1::CFP puncta (arrows) colocalized as seen in the merged image (C3).

Glutamate and Kainate Activate a Large, Rapidly Activating Current in AVA

The AVA interneurons express the GLR-1, GLR-2, and NMR-1 receptor subunits (Brockie et al., 2001a). To address whether these subunits participate in glutamatergic signaling to AVA, we recorded whole-cell currents from this interneuron in wild-type and mutant worms using patch-clamp techniques (Brockie et al., 2001b). In our dissected whole-worm preparation, the AVA neurons could be easily visualized in transgenic worms that expressed *nmr-1*::GFP. We often noticed the presence of spontaneous synaptic events (Figure 5A1), indicating that at least some synaptic communication was preserved.

To investigate glutamate-gated currents in AVA, we rapidly changed the solution near the cell by pressure application of agonists. Applying a 0.5 s pulse of 1 mM glutamate while the cell was voltage-clamped to −60mV elicited a rapidly activating inward current that subsequently inactivated in the continued presence of glutamate (Figure 5A2). The inactivation of the current was followed by a long-lasting period of desensitization when subsequent applications of glutamate no longer elicited a maximal current. Full recovery from desensitization took ~20 s. For all experiments described below, the minimal interval between glutamate applications was 30 s.

AMPA and kainate are glutamate receptor agonists that activate different subtypes of glutamate receptors

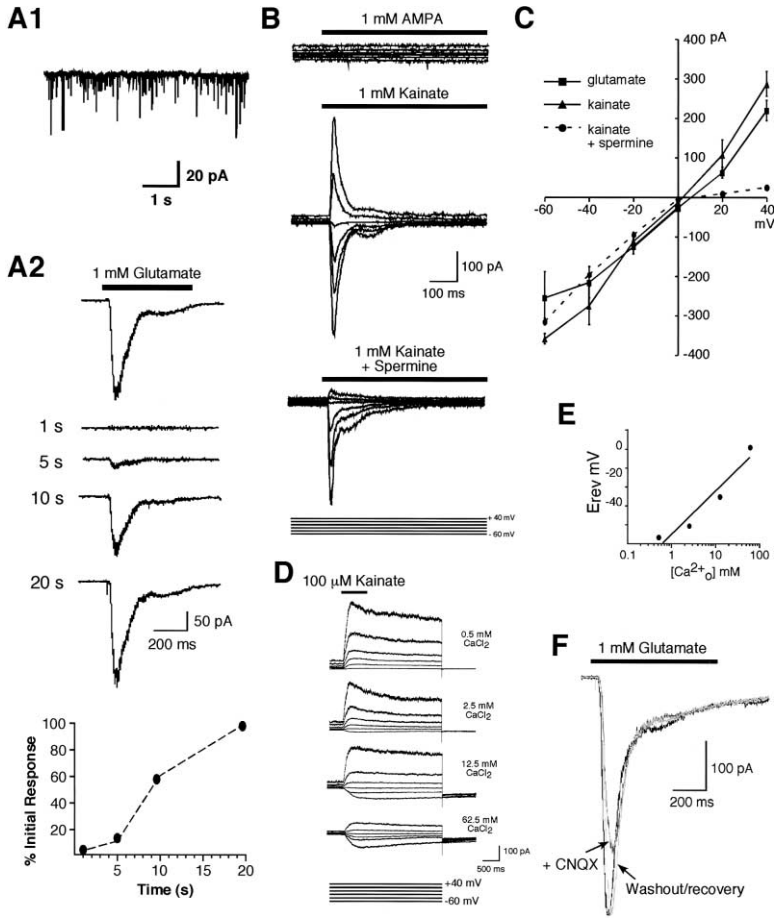

Figure 5. Characterization of Glutamate and Kainate-Gated Cation Conductances

(A1) Spontaneous synaptic activity recorded from AVA in wild-type worms. (A2) Glutamate-gated membrane currents recorded from AVA to paired applications of 1 mM glutamate (top). The second response was measured 1, 5, 10, or 20 s after the initial application. (Bottom) Percentage of the initial response versus the time interval between paired glutamate applications. (B) AMPA-gated (top) and Kainate-gated membrane currents in either the absence (middle) or presence (bottom) of 1 mM intracellular spermine (estimated free spermine, 200–300 μM). The AVA interneuron was clamped from −60mV to +40mV with voltage steps of 20mV. (C) Peak current-voltage relation for kainate-gated currents in AVA (5B) in the presence or absence of 1 mM intracellular spermine (see Experimental Procedures). Glutamate-gated currents in the absence of spermine are also shown (n = 10). (D) Kainate-gated currents recorded from AVA in Na^+ free extracellular solution that contained various concentrations of $CaCl_2$. (E) The relationship between Ca^{2+} concentration (mM) and reversal potential (mV) to kainate-evoked responses shown in (D). (F) The response to glutamate (black trace) was partially blocked by CNQX (200 μM; dark gray trace) and was fully recovered after washout of the antagonist (light gray trace).

(Dingledine et al., 1999). Whereas AMPA selectively activates receptors containing AMPA receptor subunits, kainate activates both AMPA receptors and kainate receptors. To investigate the properties of the glutamate-gated currents in AVA, the neuron was voltage clamped and stepped from −60mV to +40mV in 20mV increments, and agonist was appplied after the voltage-dependent currents decayed. No changes in transmembrane current were observed during application of 1 mM AMPA (Figure 5B). In contrast, 1 mM kainate elicited rapidly activating and inactivating currents (Figure 5B) that were similar to those observed with glutamate application. In each case, the agonist evoked a rapidly activating current that desensitized in the continued presence of agonist. These currents did not show appreciable voltage dependence, and the magnitude of the currents varied as a roughly linear function of the transmembrane potential (Figure 5C).

The current-voltage (I-V) relation for mammalian non-NMDA receptors is strongly dependent on the identity of a specific amino acid in the pore forming region of the ion channel. By a process of RNA editing, the codon encoding a glutamine (Q) may be modified so that it instead encodes an arginine (R) (Sommer et al., 1991). Unedited, Q-containing receptors show strong inward rectification that is dependent on intracellular spermine whereas edited, R-containing receptors do not (Hume et al., 1991; Bowie and Mayer, 1995). The corresponding position in *C. elegans* GLR-2 (Figure 1A; open triangle) and GLR-1 (Maricq et al., 1995) contains a glutamine, yet the glutamate-gated currents do not exhibit the expected inward rectification (Figure 5C). We hypothesized that this may be caused by dilution of intracellular spermine with the solution in the recording pipette. When we modified the intracellular recording solution to contain spermine (see Experimental Procedures), we observed dramatic inward rectification (Figures 5B and 5C) that was consistent with the rectification observed in mammalian unedited receptors (Bowie and Mayer, 1995).

Extrapolation from the linear I-V relation revealed an estimated reversal potential near 0mV. This potential suggested that the pore conductance was nonselective for cations, which is consistent with the properties of vertebrate non-NMDA ionotropic glutamate receptors (Dingledine et al., 1999). The magnitude and shape of the I-V relations for kainate and glutamate-evoked currents were approximately the same, suggesting that receptors gated by kainate provide the bulk of the rapid glutamate-gated current. Previously, we showed that *N*-methyl-D-aspartate (NMDA), a selective agonist for NMDA-type glutamate receptors, elicited a considerably smaller and slower current (Brockie et al., 2001b). This NMDA-dependent current is not activated by kainate (data not shown).

The permeability characteristics of non-NMDA glutamate receptors are also modified by RNA editing (Som-

mer et al., 1991). Unedited, Q-containing receptors are relatively Ca^{2+} permeable whereas the edited R-containing receptors have a low Ca^{2+} permeability (Hume et al., 1991), suggesting that the glutamate and kainate activated receptors in AVA might be permeable to Ca^{2+}. Ion substitution experiments revealed that Ca^{2+} could effectively substitute for Na^{+} as a charge carrier (Figure 5D). Monovalent cations were replaced with equimolar N-methyl-D-glucamine (NMDG). As the external Ca^{2+} was raised, the reversal potential for glutamate-gated currents shifted toward more positive potentials so that when the external Ca^{2+} concentration was 62.5 mM, the measured reversal potential was 1.4mV (Figure 5E). These data are consistent with the hypothesis that Ca^{2+} contributes to kainate-activated currents in AVA. Another characteristic of glutamate-gated currents that are dependent on non-NMDA receptor subtypes is their selective blockade by the competitive antagonist CNQX (Dingledine et al., 1999). We found that CNQX (200 μM) was a weak antagonist that reversibly blocked a portion of the glutamate-gated current (Figure 5F).

Glutamate-Gated Currents in the Neuron AVA Require the GLR-1 and GLR-2 Receptor Subunits

glr-1 and *glr-2* mutants are defective in avoidance responses mediated by the ASH neurons. To determine the neuronal basis for these behavioral defects, we recorded glutamate-gated currents in mutant worms. The glutamate-activated current in AVA was considerably diminished in the *glr-2* mutant (Figure 6A). However, a small, residual glutamate-gated current could still be observed. Two components were apparent in this residual current–a fast component that rapidly activated and inactivated (Figure 6A; arrow) followed by the development of a slowly activating component. The fast-activating component was dependent on *glr-2* as confirmed by recording glutamate-gated currents from transgenic *glr-2(ak10)* mutants that expressed a wild-type copy of the *glr-2* gene (Figure 6A). The currents recorded from the transgenic rescue strain were essentially indistinguishable from those recorded from wild-type worms.

As we have shown, *glr-2* mutants have a partial defect in the nose touch response. To determine how glutamate-gated currents might correlate with behavioral phenotypes, we also recorded currents from other glutamate receptor mutants (Figure 6B). In *glr-1* mutants, essentially all of the rapidly activating current was eliminated, including the small, rapid component observed in *glr-2* mutants. The currents recorded from AVA in the double mutant *glr-2 glr-1* were indistinguishable from those recorded in *glr-1* mutants. The small, slowly developing current that remained in the *glr-2 glr-1* double mutant was not observed in the *nmr-1; glr-2 glr-1* triple mutant, indicating that this was the NMDA-activated component. In *glr-1* and *glr-2* mutants and the *glr-2 glr-1* double mutant, the peak current I-V relation was outwardly rectifying (Figure 6C). This is typical of NMDA-gated currents and suggests that this remaining current is mediated by receptors that contain the NMR-1 subunit. The shape of the I-V relation was restored in *glr-2(ak10)* transgenic mutants that expressed the wild-type *glr-2* gene (Figure 6C).

Kainate-evoked currents were absent in the *glr-1* and *glr-2* mutants, and the *glr-2 glr-1* double mutants (data not shown). The small, fast current observed in *glr-2* mutants was only observed with glutamate application (data not shown), suggesting that GLR-2 may be required for kainate binding or function. Together, the data described above suggest that (1) the majority of the glutamate-gated current in AVA is dependent on kainate receptors formed by a heteromeric complex containing GLR-1 and GLR-2, and (2) the bulk of the residual current observed in the absence of GLR-1 and GLR-2 is mediated by the NMR-1 subunit.

We suspected that the magnitude of the small, fast current component observed in *glr-2* mutants was altered by receptor desensitization. To better study this current, we recorded glutamate-gated currents from transgenic *glr-2 glr-1* mutants that expressed a variant of GLR-1 that contained a mutation that greatly reduces receptor desensitization (GLR-1[Q/Y]) (Stern-Bach et al., 1998; Brockie et al., 2001b). Glutamate-activated currents in the transgenic mutants that expressed GLR-1(Q/Y) (Figure 6B) were far longer lived and larger in amplitude than those observed in *glr-2* mutants that expressed wild-type GLR-1 (Figure 6A), suggesting that the apparent magnitude of the GLR-2 independent current was underestimated by the kinetics of exogenous glutamate application. The effect of GLR-1(Q/Y) was also apparent in transgenic *nmr-1; glr-2 glr-1* triple mutants (Figure 6B). These results suggest that GLR-1 is a component of a receptor complex that mediates the rapid current component observed in *glr-2* mutants and that GLR-1 contributes to the kinetics of desensitization. The GLR-1(Q/Y) variant was also used to test the hypothesis that our failure to record AMPA-gated currents in the AVA neurons was secondary to the fast desensitization kinetics characteristic of AMPA receptors (Dingledine et al., 1999). We were still not able to record AMPA-gated currents in transgenic worms that expressed GLR-1(Q/Y) (data not shown).

Because the majority of the glutamate-activated current is dependent on both the GLR-1 and GLR-2 receptor subunits, we sought to determine which subunit was the primary determinant of the rate of desensitization by examining glutamate-gated currents in transgenic mutants that expressed GLR-2(Q/Y)–a variant of GLR-2 that had a glutamine to tyrosine substitution analogous to that introduced in GLR-1(Q/Y) (Figure 1A). We recorded currents from AVA in transgenic mutants that substituted GLR-1(Q/Y) for GLR-1, GLR-2(Q/Y) for GLR-2, or both variants for GLR-1 and GLR-2. Glutamate-gated currents recorded from transgenic *glr-2* mutants that expressed GLR-2(Q/Y) rapidly desensitize (Figure 6D). Furthermore, the kinetics of desensitization in *glr-2 glr-1* transgenic mutants that expressed both GLR-1(Q/Y) and GLR-2(Q/Y) were not substantially different from *glr-1* mutants that expressed GLR-1(Q/Y) alone (Figure 6D).

We have previously shown that defects in glutamatergic signaling lead to a change in the amount of time a worm spends moving forward as it explores or forages in its environment. (Brockie et al., 2001b). To determine the behavioral consequences of modifying the desensitization kinetics of glutamate-gated currents, we measured the average duration of forward movement in transgenic worms that expressed GLR-1(Q/Y). Com-

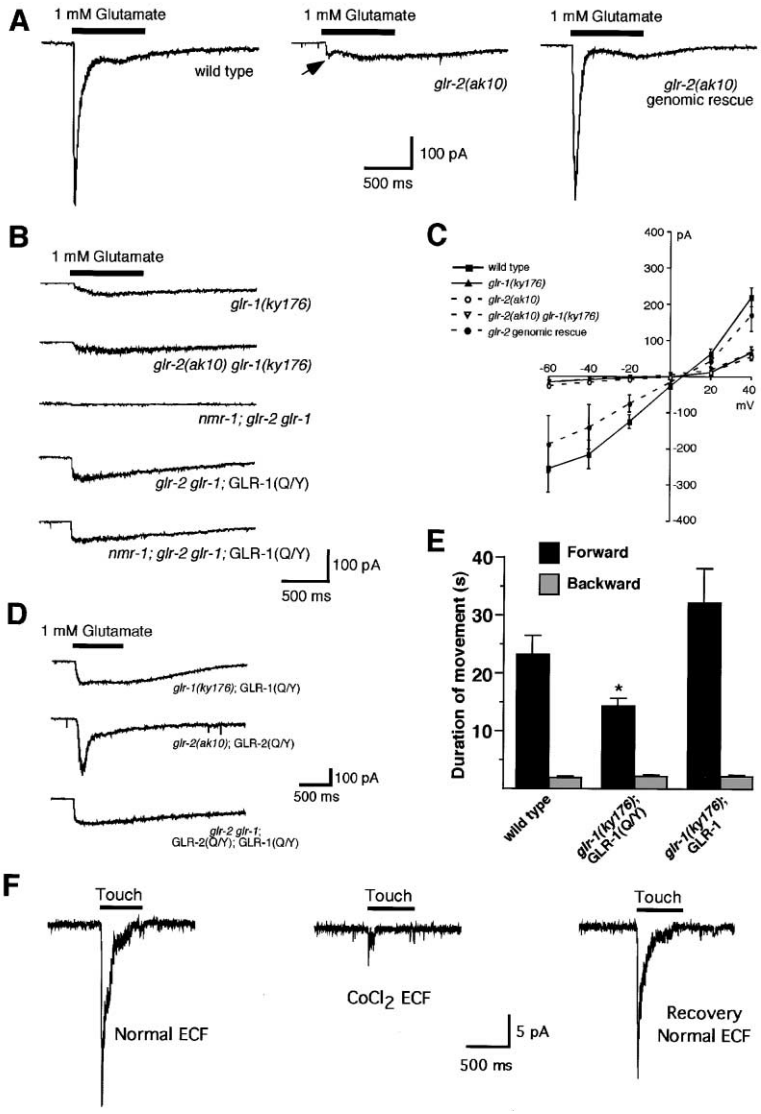

Figure 6. Rapidly Activating Glutamate-Gated Currents from AVA Are Dependent on *glr-2* and *glr-1*

(A) Glutamate-gated currents in wild-type worms (left) and *glr-2* mutants (middle). Note the small, rapidly activating and inactivating current component in the *glr-2* mutant (arrow). The larger, rapid current component lacking in *glr-2(ak10)* was restored in transgenic mutants that expressed a *glr-2* genomic clone (right). In (A), (B), (D), and (F), the neuron was held at −60mV. (B) Glutamate-gated currents recorded from *glr-1*, *glr-2 glr-1* double and *nmr-1; glr-2 glr-1* triple mutants. Nondesensitizing glutamate-gated currents from transgenic *glr-2 glr-1* double and *nmr-1; glr-2 glr-1* triple mutants that expressed GLR-1(Q/Y) are also shown. (C) Current-voltage relation for peak glutamate-gated currents in wild-type worms (n = 10), *glr-1* (n = 6), and *glr-2* (n = 10) mutants; *glr-2 glr-1* double mutants (n = 9); and *glr-2* transgenic mutants that expressed a *glr-2* wild-type genomic clone (n = 3). (D) Glutamate-gated currents recorded from transgenic mutants that expressed either GLR-1(Q/Y) (top), GLR-2(Q/Y) (middle), or both (bottom). (E) Average duration of forward and backward movement in wild-type worms (n = 10), and transgenic *glr-1* mutants that overexpressed either GLR-1(Q/Y) (n = 10) or wild-type GLR-1 (n = 10). *Statistically different from wild-type ($p < 0.03$). (F) Tactile-evoked responses in AVA of a wild-type worm in either the absence (left) or presence (middle) of $CoCl_2$. The evoked response could be recovered by washing out $CoCl_2$ from the extracellular fluid (right). The black bar indicates the period when a glass rod was used to gently touch the worm's nose.

pared to wild-type worms or transgenic worms that overexpressed the native GLR-1 receptor, the average duration of forward movement in worms that expressed GLR-1(Q/Y) was significantly shortened (Figure 6E). Thus, the kinetics of glutamate receptor desensitization can be directly related to a quantitative behavior.

Mechanical Stimulation Evokes Synaptic Currents in AVA

To address how mechanosensory information is transmitted by ASH, we recorded from AVA while applying a mechanical stimulus. When AVA was voltage-clamped at −60mV, a brief touch of a glass rod to the worm's nose elicited a rapidly activating current that then inactivated (Figure 6F). The kinetics of the current response were similar to that observed with exogenous application of glutamate. Both the current evoked by tactile stimulation and spontaneous synaptic events were dependent on external Ca^{2+} as shown by the blockade observed with replacement of external Ca^{2+} with Co^{2+} (Figure 6F). This result suggests that the tactile-evoked current was dependent on the synaptic release of neurotransmitter. In wild-type worms, 26 of the 43 trials evoked a response. We suspect that the failure rate reflects damage to the neural circuitry during dissection. We were able to record evoked currents from AVA in 17 glutamate receptor mutants–either *glr-1* or the *glr-2 glr-1* double mutant. We found that in seven of these experiments, tactile stimulation still evoked a small current response, suggesting that other synaptic inputs in addition to ASH may have been activated by the tactile stimulus. Our results show the feasibility of directly studying neural synaptic transmission in *C. elegans* but indicate that definitive analyses await the development of pharmacological agents that effectively block specific currents.

Mutations in *egl-3* Suppress both the Mechanosensory and Osmotic Avoidance Defects in *glr-1* Mutants in an *nmr-1*-Dependent Manner

A recent study has shown that mutations in the *egl-3* gene suppress the nose touch defect in *glr-1* mutants (Kass et al., 2001). *egl-3* encodes a member of the PC2

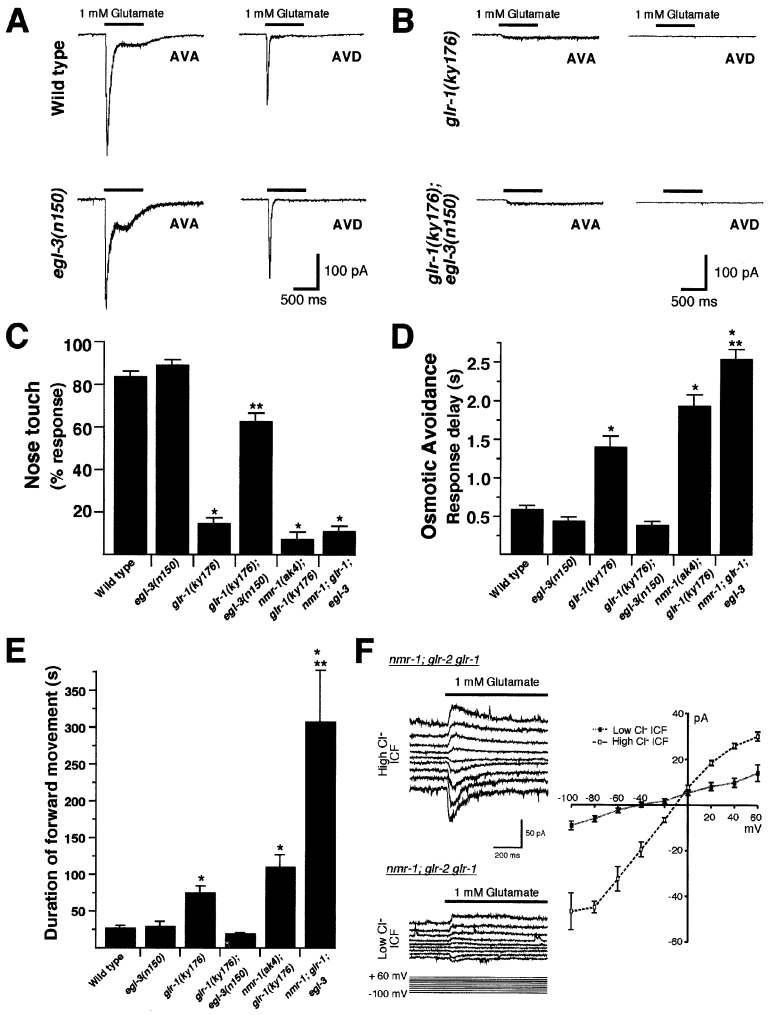

Figure 7. *egl-3(n150)* Suppression of *glr-1(ky176)* Is Dependent on *nmr-1* and Does Not Affect Postsynaptic Glutamate Receptors

(A) Glutamate-gated currents in the AVA and AVD interneurons of wild-type worms (top) and *egl-3* mutants (bottom). Following the initial peak current, a secondary current component was observed. The origin of this component is not known and its magnitude varies considerably from cell to cell independent of *egl-3*. (B) Glutamate-gated currents in the AVA and AVD interneurons of *glr-1* mutants (top) and *glr-1; egl-3* double mutants (bottom). In (A) and (B), interneurons were held at −60mV. (C) The percentage response to ten consecutive nose touch trials in wild-type (n = 9), *egl-3* (n = 9), *glr-1* (n = 9), *glr-1; egl-3* (n = 12), *nmr-1; glr-1* (n = 10), and *nmr-1; glr-1; egl-3* (n = 10) mutants. Statistically different from wild-type (*) or *glr-1* (**); ($p < 0.01$). (D) The delay in the response to osmotic stimuli in wild-type (n = 44), *egl-3* (n = 30), *glr-1* (n = 35), *glr-1; egl-3* (n = 46), *nmr-1; glr-1* (n = 43), and *nmr-1; glr-1; egl-3* (n = 42) mutants. Only worms that responded to the stimulus were included in the delay analysis. 100% of wild-type worms, *glr-1* and *egl-3* mutants, and *glr-1; egl-3* double mutants responded to the fructose. Of the *nmr-1; glr-1* double mutants and *nmr-1; glr-1; egl-3* triple mutants screened, 9 in 54 double and 60 in 102 triple mutants did not respond. Statistically different from wild-type (*; $p < 0.01$) or *nmr-1(ak4); glr-1(ky176)* (**; $p < 0.02$). (E) Foraging behavior. The average duration of forward movement in wild-type (n = 12), *egl-3* (n = 12), *glr-1* (n = 22), *glr-1; egl-3* (n = 10), *nmr-1; glr-1* (n = 22), and *nmr-1; glr-1; egl-3* (n = 10) mutants. Statistically different from wild-type (*) or *nmr-1(ak4); glr-1(ky176)* (**); ($p < 0.01$). (F) Glutamate-gated currents recorded from *nmr-1; glr-2 glr-1* triple mutants. (Left) Currents recorded from the triple mutant using an intracellular fluid (ICF) with either a high (top) or low (bottom) Cl^- concentration. (Right) Current-voltage relation for glutamate-gated currents recorded from triple mutants using either high (n = 3) or low (n = 3) Cl^- ICF.

family of proprotein convertases thought to be required for the function of specific neuropeptides. Transgenic *glr-1; egl-3* mutants that expressed a wild-type copy of *egl-3* in the postsynaptic targets of ASH, including AVA and AVD, were no longer suppressed and had mechanosensory defects similar to *glr-1* mutants. These results suggest that EGL-3 functions postsynaptically to modify glutamatergic neurotransmission (Kass et al., 2001). To directly test this, we recorded glutamate-gated currents in *egl-3(n150)* and *glr-1(ky176); egl-3(n150)* double mutants in AVA and AVD–two interneurons that are required for the backward escape response. Glutamate-gated currents recorded from either AVA or AVD in *egl-3* and *glr-1; egl-3* mutants were similar to wild-type and *glr-1* mutants, respectively (Figures 7A and 7B). This finding demonstrated that the mutation in *egl-3* did not restore glutamate-gated currents in *glr-1* mutants by, for example, upregulating postsynaptic glutamate receptors and suggested that EGL-3 might function to modulate glutamatergic signaling from ASH.

EGL-3 may normally function to reduce the concentration of released glutamate at ASH-interneuron synapses by either downregulating glutamate release or by upregulating glutamate transport from the synaptic cleft. For either of these possibilities, mutations in *egl-3* would result in higher levels of glutamate that may be sufficient to activate NMDA receptors, thereby restoring the mechanosensory response in *glr-1* mutants. To test this hypothesis, we determined whether the nose touch response in *glr-1; egl-3* double mutants was dependent on *nmr-1*. In contrast to the normal nose touch response of *glr-1; egl-3* double mutants, *nmr-1; glr-1; egl-3* triple mutants were nose touch defective (Figure 7C). Thus, the *egl-3* suppression of *glr-1* was absolutely dependent on *nmr-1* function. We also tested the role of *egl-3* in osmotic avoidance behavior. Using the assay described earlier (Figure 3A), we demonstrated that *egl-3(n150)* suppressed the osmotic avoidance defect of *glr-1* mutants, but not of *nmr-1; glr-1* double mutants (Figure 7D). *nmr-1* expression is limited to a small subset of interneurons, most of which are targets of ASH. Thus, nose touch and osmotic stimuli must activate NMDA receptors in the *glr-1; egl-3* double mutant.

A Glutamate-Gated Chloride Current Is Also Present in AVA

We have previously shown that mutations in both *nmr-1* and *glr-1* reduce the frequency of reversals during forag-

ing behavior (Brockie et al., 2001b). Here, we show that mutations in *egl-3* also suppress the foraging defects of *glr-1* mutants, but not of *nmr-1; glr-1* double mutants (Figure 7E). Interestingly, the defects of the *nmr-1; glr-1; egl-3* triple mutant were more severe than those of the *nmr-1; glr-1* double mutant in both osmotic avoidance and foraging behavior. The delay in response to the osmotic stimulus was significantly greater in the triple mutant compared to the *nmr-1; glr-1* double mutant ($p < 0.01$). In fact, 59% of the *nmr-1; glr-1; egl-3* mutants did not respond to the stimulus and moved through the fructose spot. To address this finding, we characterized the electrophysiological properties of the AVA interneuron in *nmr-1; glr-2 glr-1* mutants. In the absence of functional non-NMDA and NMDA receptors, glutamate perfusion could elicit a small inward current when AVA was clamped at hyperpolarizing potentials (Figure 7F). In contrast with the previously discussed glutamate-gated currents, which reversed polarity near 0mV (Figure 5C), this small residual current reversed polarity at ~ -40mV. Because the estimated reversal potential for a chloride-permeable channel was ~ -48mV, we reasoned that the residual current might have been due to a glutamate-activated chloride conductance. Under conditions of increased intracellular Cl^-, glutamate application resulted in a larger current, which we estimated to reverse at ~ -11mV–close to the calculated reversal potential for Cl^- (-10mV). These results are consistent with the presence of a glutamate-gated chloride conductance in AVA. Glutamate-gated chloride currents are mediated by receptors that are related to ionotropic acetylcholine and GABA receptors. Several subunits have been identified and they appear to have differential expression in muscles and the nervous system (Dent et al., 2000). Perhaps glutamate-gated chloride channels function in the locomotory control circuit to help reestablish forward movement following a backward avoidance response.

Discussion

In *C. elegans*, it has been recognized that the ASH polymodal sensory neurons differentially transmit aversive stimuli (Bargmann and Kaplan, 1998). We have now shown that the non-NMDA glutamate receptor subunits GLR-1 and GLR-2 are necessary for the avoidance of both mechanical and osmotic stimuli and that the NMDA subunit NMR-1 plays a role in the detection of osmotic stimuli, but not mechanical stimuli. Electrophysiological analysis in *glr-1*, *glr-2*, and *nmr-1* mutants has enabled us to correlate the behavioral defects with altered electrophysiological properties in the AVA interneuron, a postsynaptic target of ASH sensory neurons. Our data suggest that synaptic decoding of modality specific signals is likely achieved by the differential activation of postsynaptic non-NMDA and NMDA receptors.

GLR-2 Is Required for Mechanosensory Signaling

To address how glutamate receptor subunits contribute to ASH signaling, we generated a deletion mutation in the *glr-2* gene. We showed that the nose touch avoidance response in *glr-2* mutants was approximately intermediate between that of wild-type worms and *glr-1* mutants, and that the defect of the *glr-2 glr-1* double mutant was no greater than that of the *glr-1* mutant alone. Interestingly, the measured glutamate-activated currents in the AVA interneurons could explain the distinct behavioral phenotypes of the *glr-1* and *glr-2* mutants. In *glr-1* mutants, essentially all of the non-NMDA dependent current was eliminated, whereas in *glr-2* mutants a residual, GLR-1-dependent current was still present. These results suggest that GLR-1 and GLR-2 function together in a heteromeric complex that mediates most of the non-NMDA dependent current activated by exogenous glutamate application and that GLR-1 can also function independently of GLR-2. We conclude that the residual GLR-1-dependent glutamate-gated current observed in *glr-2* mutants is sufficient to partially mediate a response to tactile stimuli to the worm's nose.

Characteristics of GLR-1- and GLR-2-Dependent Currents

In vertebrates, non-NMDA receptor subunits are categorized based on molecular and pharmacological criteria into AMPA and kainate subtypes. Both subtypes rapidly desensitize in the continued presence of glutamate, but AMPA receptors recover from desensitization roughly 10-fold faster than kainate receptors (Dingledine et al., 1999). Most AMPA receptors have a nonaromatic residue in a conserved position of a ligand binding region (L507), whereas kainate receptors have an aromatic residue (Y521) (Stern-Bach et al., 1998). Like vertebrate kainate receptors, the GLR-1-/GLR-2-dependent current in AVA desensitized when activated by kainate. Moreover, the recovery from desensitization took $\sim$20 s–over an order of magnitude slower than that observed for vertebrate AMPA receptors (Dingledine et al., 1999). However, both GLR-1 and GLR-2 have a nonaromatic glutamine residue, characteristic of AMPA receptor subtypes, in the conserved position corresponding to L507 or Y521. When this residue in GLR-1 was changed to tyrosine, a marked difference in the kinetics of desensitization was detected in transgenic worms. The decreased rate of desensitization also led to an easily detected change in foraging behavior, demonstrating that control of glutamate receptor desensitization rate could have important consequences for how a worm navigates its environment.

In vertebrate non-NMDA receptors, Ca^{2+} permeability is regulated by a key glutamine (Q) residue in the pore-forming region of specific receptor subunits. Thus, when the vertebrate GluR2 mRNA is posttranscriptionally edited to encode an arginine (R) residue, the permeability to Ca^{2+} is considerably reduced and the I-V relation changes from inwardly rectifying to linear (Hume et al., 1991; Sommer et al., 1991). In *C. elegans*, the glutamate-gated current could be carried by Ca^{2+} and, in the presence of intracellular spermine, the I-V relation for glutamate-gated currents in AVA was inwardly rectifying, consistent with the Q form of the receptor in *C. elegans*. Our results suggest that glutamatergic neurotransmission mediated by GLR-1 and GLR-2 may cause an increase in the intracellular Ca^{2+} concentration of postsynaptic targets.

GLR-1, GLR-2, and NMR-1 Are Required for Osmotic Signaling

We have shown that both tactile and osmotic signaling via the ASH sensory neurons are dependent on the non-

NMDA receptor subunits GLR-1 and GLR-2. Interestingly, although we found no evidence that NMDA receptors are required for the nose touch response, we did observe a role for the NMR-1 subunit in osmotic avoidance behavior. The role of NMR-1 in this response may be to facilitate temporal summation of synaptic inputs, thus leading to an avoidance response (Brockie et al., 2001b). We found that the osmotic avoidance defect of the *nmr-1; glr-2 glr-1* triple mutant was less severe than that observed in *eat-4* mutants, suggesting that other glutamate-gated currents may contribute to the behavior.

To directly test whether glutamatergic signaling mediated the nose touch response, we gently moved a glass pipette against the nose of the worm while simultaneously recording whole-cell currents from AVA. This current could be blocked by Co^{2+}, indicating it is likely of synaptic origin. Although the high failure rate associated with this technique prevented a significant mutant analysis of the response, the future use of pharmacological agents that block receptor-dependent currents should increase the power of this approach to the study of synaptic function in *C. elegans*.

Decoding Modality-Specific Sensory Information Detected by the ASH Sensory Neurons

How does the nervous system decode modality-specific sensory information? To distinguish between mechanosensory and osmotic stimuli, the ASH sensory neurons may release distinct levels of neurotransmitter or may utilize multiple signaling molecules. Either of these possibilities would lead to modality-specific activation of a distinct subset of postsynaptic receptors. By demonstrating that the response to mechanical versus osmotic stimuli have a distinct dependence on non-NMDA and NMDA receptor subtypes, we provide evidence that polymodal signaling is likely achieved by the differential activation of these receptor subtypes. Thus, tactile and osmotic stimuli are predicted to activate the OSM-9 receptor required for the detection of both sensory modalities (Colbert et al., 1997) but result in different degrees or durations of depolarization. This, in turn, would lead to modality-specific levels of neurotransmitter release that activate only non-NMDA glutamate receptor subtypes (nose touch stimuli) or both non-NMDA and NMDA receptors (osmotic stimuli).

How might changes in the levels of released glutamate activate different subsets of postsynaptic glutamate receptors? In previous studies, we have shown that GLR-1 and NMR-1 are likely to be differentially distributed at postsynaptic sites with GLR-1 localized at the synapse and NMR-1 situated at extrasynaptic sites (Brockie et al., 2001b). Our present results suggest a model where osmotic stimuli, but not nose touch stimuli, result in the release of glutamate that is sufficient to activate both synaptic non-NMDA receptors and extrasynaptic NMDA receptors (Figure 8). This model was supported by the observation that suppression of the behavioral defects of *glr-1* mutants by mutations in *egl-3* is dependent on *nmr-1*. Because *nmr-1* expression is limited to an extremely small subset of the nervous system that includes the AVA and AVD interneuron targets of ASH (Brockie et al., 2001a), it is plausible that *egl-3* controls

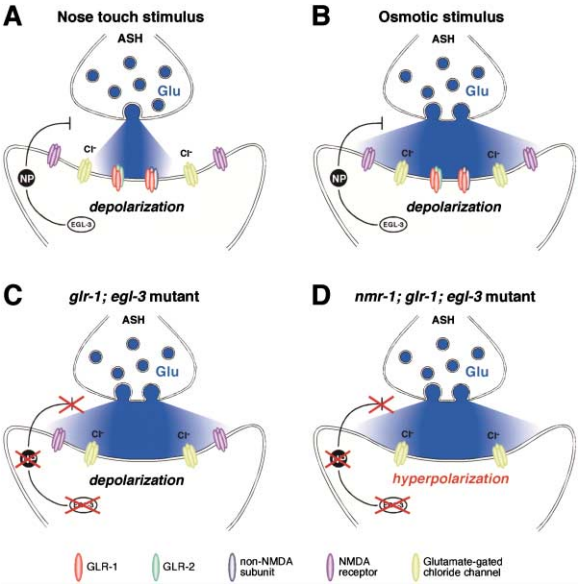

Figure 8. Differential Activation of Non-NMDA and NMDA Glutamate Receptors Mediate the Response to Mechanical versus Osmotic Stimuli

(A) Mechanical and (B) osmotic stimuli detected by the ASH sensory neurons evoke different levels of glutamate release (blue). The concentration of synaptic glutamate in response to osmotic stimuli is sufficient to activate extrasynaptic NMDA receptors whereas mechanical stimuli only activate synaptic non-NMDA receptors. EGL-3 activates an unidentified neuropeptide (NP) that downregulates the concentration of synaptic glutamate. The placement of non-NMDA and glutamate-gated Cl^- receptors is arbitrary. (C) In the absence of EGL-3, the concentration of released glutamate in response to either mechanical and osmotic stimuli is sufficient to activate extrasynaptic NMDA receptors such that *glr-1; egl-3* mutants show normal ASH-dependent avoidance behaviors. (D) In the absence of both NMDA and non-NMDA receptors, the increase in glutamate that results from mutations in *egl-3* does not restore avoidance behaviors. As a result of the absence of glutamate-gated cationic conductances, glutamate now exclusively activates glutamate-gated chloride channels. This causes a hyperpolarization of the locomotory interneurons, leading to a decreased probability of reversing backward and consequently a strong bias toward forward movement.

synaptic communication between ASH and these interneurons.

EGL-3 belongs to the PC2 family of proprotein convertases that process proneuropeptides into active signaling molecules (Kass et al., 2001). In some cases, neuropeptides function as neuromodulators that can influence the levels of neurotransmitter release (Akopian et al., 2000; Silva et al., 2001). Thus, EGL-3 might indirectly affect glutamatergic signaling by activating an unidentified neuropeptide that inhibits stimulus-evoked glutamate release from ASH. Neuropeptides have also been shown to downregulate postsynaptic currents leading to a depression of synaptic activity (Gao and van den Pol, 2001). Therefore, neuropeptides processed by EGL-3 may function postsynaptically to downregulate glutamate receptors. To distinguish between these two hypotheses, we showed that mutations in *egl-3* did not affect the postsynaptic response to exogenously applied glutamate in either AVA or AVD interneurons, suggesting a presynaptic role for EGL-3. It is possible

that we were unable to detect small changes in current amplitude, although we have shown that we can record currents in the 10–20 pA range. Alternatively, mutations in *egl-3* may cause subtle changes in receptor kinetics or membrane potential that were not uncovered by our recording techniques.

We suggest that mutations in *egl-3* may cause an increase in the concentration of synaptic glutamate. Thus, the normal function of *egl-3* may be to downregulate presynaptic neurotransmitter release via an unidentified neuropeptide or upregulate glutamate transport from the synaptic cleft (Figure 8). Our analysis of the glutamate-gated chloride conductance in AVA provides additional support for this hypothesis. During foraging behavior, *glr-1* mutants move forward for longer durations than wild-type worms. This defect is suppressed by the mutation in *egl-3*. However, the opposite effect on forward duration is observed when the NMR-1 subunit is also mutated. Now, rather than having a suppressive effect, the mutation in *egl-3* enhances the behavioral defect such that the duration of forward movement in *nmr-1; glr-1; egl-3* triple mutants is much longer than that observed in the *nmr-1; glr-1* double mutant. In the absence of *nmr-1* and *glr-1*, all glutamate-gated cationic depolarizing currents are eliminated in AVA. Our model predicts that mutations in *egl-3* now lead to the exclusive activation of glutamate-gated chloride channels, thereby hyperpolarizing neurons in the locomotory control circuit. Presumably, this would promote movement in a forward direction since mutations that act to depolarize these interneurons lead to the activation of backward movement (Zheng et al., 1999). Thus, *egl-3* has opposite effects on the duration of forward movement that are dependent on the complement of postsynaptic glutamate receptors. These results are most consistent with *egl-3* influencing the concentration of synaptic glutamate and cannot be easily explained by a nonspecific effect of *egl-3* on postsynaptic excitability.

Other examples have been described where differential activation of non-NMDA and NMDA receptors may facilitate the decoding of sensory information. Studies of nociception in the adult rat spinal cord suggest that differential activation of synaptic non-NMDA and extrasynaptic NMDA receptors can distinguish between acute and chronic pain (Momiyama, 2000). In the retina, spontaneous release of neurotransmitter at ganglion cell synapses elicits only a non-NMDA-dependent current. In contrast, evoked release results in the activation of both NMDA and non-NMDA receptors. The NMDA component can also be elicited by application of drugs that reduce the uptake of extracellular glutamate (Chen and Diamond, 2002). These results provide functional evidence for spatial segregation of non-NMDA and NMDA receptors and suggest that NMDA receptors may amplify the response to strong light compared to weak light stimulation. In *C. elegans,* we were able to use a combination of genetic, behavioral, and electrophysiological analyses to test whether differential activation of non-NMDA and NMDA glutamate receptors contribute to polymodal signaling by the ASH sensory neurons. Our analysis of specific avoidance behaviors in *C. elegans* may help to uncover the mechanisms of polymodal signaling such as nociception in more complex organisms.

Experimental Procedures

Strains

Nematodes were raised at 20°C under standard laboratory conditions on agar plates cultured with the *Escherichia coli* strain OP50. Wild-type nematodes were *C. elegans* strain N2. Transgenic strains were generated by microinjection into the gonad of adult hermaphrodite worms to achieve germline transformation. Transformants were selected by injecting worms with the plasmid pPB1 and isolating those that expressed GFP. Alternatively, *lin-15(n765ts)* mutants were coinjected with a *lin-15* rescuing plasmid (pJM23) and transformants were identified as non-Muv adult hermaphrodites (Maricq et al., 1995).

Molecular Biology and Genetics

The *glr-2* cDNA was isolated by PCR amplification from *C. elegans* first strand cDNA. The g*lr-2* genomic clone pPB57 was isolated from cosmids BO28O and KO4G7. An ~10 kb XhoI fragment was subcloned into Bluescript SK+ (Stratagene). The following additional plasmids were used: pPB53, CFP was inserted into a HindIII site of the *glr-1* genomic clone (GLR-1::CFP); pV1 (Maricq et al., 1995); pPB60, YFP was inserted into an XmaI site 32 codons upstream of the *glr-2* stop codon in pPB57 (GLR-2::YFP); pPB66, sequences amplified from *glr-2* were inserted into pPD114.108 (a gift from A. Fire) generating GFP::GLR-2; pPB58 encodes GLR-1(Q/Y) (Brockie et al., 2001b); pPB59 encodes GLR-2(Q/Y) generated by site directed mutagenesis to produce a point mutation (Q580Y) in GLR-2.

The Tc1 transposon insertion in the *glr-2* 3′ UTR was detected by PCR using procedures previously described (Maricq et al., 1995). Subsequent deletion in the *glr-2* loci was generated by imprecise excision of Tc1.

Behavioral Assays

The osmotic avoidance ring assay (Culotti and Russell, 1978) and the nose touch assay (Kaplan and Horvitz, 1993) were performed as previously described (Brockie et al., 2001b). To determine the delay in the response to osmotic stimuli, we used an alternative assay to that described above (Hilliard et al., 2002). A young adult worm was transferred without food to an agar plate and allowed to recover for at least 2 min. A small drop of 1 M fructose in control buffer (30 mM Tris [pH 7.5], 100 mM NaCl, 10 mM KCl) was then placed in the path of the worm as it moved forward. The response was recorded using a Sony Digital Video Camera Recorder and the time interval (delay) between the initial contact with the solution and the response (backward movement) was determined. The response to the control buffer was also determined. Foraging behavior was characterized as previously described (Zheng et al., 1999; Brockie et al., 2001b). In all figures, error bars indicate the standard error of the mean (SEM).

Electrophysiology

In vivo recordings from identified neurons were performed as previously described (Brockie et al., 2001b). Solutions: intracellular fluid (ICF) was composed of the following: 115 mM K-gluconate, 25 mM KCl, 50 mM HEPES, 0.1 mM $CaCl_2$, 1 mM BAPTA, 5 mM MgATP, 0.5 mM NaGTP, 0.5 mM cAMP, 0.5 mM cGMP (pH 7.35, adjusted with KOH). Sucrose was added to adjust the osmolarity to 335 mOsm. High Cl^- ICF: same as ICF with the following changes: 25 mM K-gluconate and 115 mM KCl. Spermine ICF: ICF with 1 mM spermine. Because ATP buffers spermine, the estimated free spermine concentration is ~200–300 μM (Watanabe et al., 1991). Extracellular fluid (ECF) was composed of 150 mM NaCl, 5 mM KCl, 5 mM $CaCl_2$, 1 mM $MgCl_2$, 15 mM HEPES, and 10 mM Glucose (pH 7.35, adjusted with NaOH). Sucrose was added to adjust the osmolarity to 340 mOsm. Calcium permeability: equimolar NMDG was substituted for NaCl and KCl. $CaCl_2$ was added at the expense of NMDG (pH 7.35, adjusted with HCl). Osmolarity adjusted with sucrose as above. Agonists in ECF were pressure ejected using a Picospritzer II (General Valve Corporation) or an ALA Scientific BPS-4 pressurized valve control system. Antagonists in ECF were bath applied.

Evoked response: tactile stimulation was achieved by applying

brief hits to multiple areas of the nose using a glass pipette controlled by a Burleigh PZ100 Step Driver.

Acknowledgments

We thank M. Vetter and members of the Maricq laboratory for comments on the manuscript and Peter Seeburg for suggestions about the electrophysiological analysis. We would like to thank the *Caenorhabditis* Genetics Center (funded by the National Institutes of Health) for providing worm strains. This research was supported in part by NSF CAREER Award 9876262, the Sloan Foundation, the Burroughs Wellcome Foundation, and by grant NS35812 from the National Institutes of Health.

Received: April 15, 2002
Revised: October 4, 2002

References

Akopian, A., Johnson, J., Gabriel, R., Brecha, N., and Witkovsky, P. (2000). Somatostatin modulates voltage-gated K(+) and Ca(2+) currents in rod and cone photoreceptors of the salamander retina. J. Neurosci. *20*, 929–936.

Bargmann, C.I., and Kaplan, J.M. (1998). Signal transduction in the Caenorhabditis elegans nervous system. Annu. Rev. Neurosci. *21*, 279–308.

Bellocchio, E.E., Reimer, R.J., Fremeau, R.T., Jr., and Edwards, R.H. (2000). Uptake of glutamate into synaptic vesicles by an inorganice phosphate transporter. Science *289*, 957–960.

Berger, A.J., Hart, A.C., and Kaplan, J.M. (1998). G alphas-induced neurodegeneration in Caenorhabditis elegans. J. Neurosci. *18*, 2871–2880.

Bowie, D., and Mayer, M.L. (1995). Inward rectification of both AMPA and kainate subtype glutamate receptors generated by polyamine-mediated ion channel block. Neuron *15*, 453–462.

Brockie, P.J., Madsen, D.M., Zheng, Y., Mellem, J., and Maricq, A.V. (2001a). Differential expression of glutamate receptor subunits in the nervous system of *C. elegans* and their regulation by the homeodomain protein UNC-42. J. Neurosci. *21*, 1510–1522.

Brockie, P.J., Mellem, J.E., Hills, T., Madsen, D.M., and Maricq, A.V. (2001b). The C. elegans glutamate receptor subunit NMR-1 is required for slow NMDA-activated currents that regulate reversal frequency during locomotion. Neuron *31*, 617–630.

Chalfie, M., Sulston, J.E., White, J.G., Southgate, E., Thomson, J.N., and Brenner, S. (1985). The neural circuit for touch sensitivity in Caenorhabditis elegans. J. Neurosci. *5*, 956–964.

Chen, S., and Diamond, J.S. (2002). Synaptically released glutamate activates extrasynaptic NMDA receptors on cells in the ganglion cell layer of rat retina. J. Neurosci. *22*, 2165–2173.

Colbert, H.A., Smith, T.L., and Bargmann, C.I. (1997). OSM-9, a novel protein with structural similarity to channels, is required for olfaction, mechanosensation, and olfactory adaptation in Caenorhabditis elegans. J. Neurosci. *17*, 8259–8269.

Culotti, J.G., and Russell, R.L. (1978). Osmotic avoidance defective mutants of the nematode *Caenorhabditis elegans*. Genetics *90*, 243–256.

Dent, J.A., Smith, M.M., Vassilatis, D.K., and Avery, L. (2000). The genetics of ivermectin resistance in Caenorhabditis elegans. Proc. Natl. Acad. Sci. USA *97*, 2674–2679.

Dingledine, R., Borges, K., Bowie, D., and Traynelis, S.F. (1999). The glutamate receptor ion channels. Pharmacol. Rev. *51*, 7–61.

Gao, X.B., and van den Pol, A.N. (2001). Melanin concentrating hormone depresses synaptic activity of glutamate and GABA neurons from rat lateral hypothalamus. J. Physiol. (Lond.) *533*, 237–252.

Hart, A.C., Sims, S., and Kaplan, J.M. (1995). Synaptic code for sensory modalities revealed by C. elegans GLR-1 glutamate receptor. Nature *378*, 82–85.

Hart, A.C., Kass, J., Shapiro, J.E., and Kaplan, J.M. (1999). Distinct signaling pathways mediate touch and osmosensory responses in a polymodal sensory neuron. J. Neurosci. *19*, 1952–1958.

Hilliard, M.A., Bargmann, C.I., and Bazzicalupo, P. (2002). C. elegans responds to chemical repellents by integrating sensory inputs from the head and the tail. Curr. Biol. *12*, 730–734.

Hume, R.I., Dingledine, R., and Heinemann, S.F. (1991). Identification of a site in glutamate receptor subunits that controls calcium permeability. Science *253*, 1028–1031.

Julius, D., and Basbaum, A.I. (2001). Molecular mechanisms of nociception. Nature *413*, 203–210.

Kaplan, J.M., and Horvitz, H.R. (1993). A dual mechanosensory and chemosensory neuron in Caenorhabditis elegans. Proc. Natl. Acad. Sci. USA *90*, 2227–2231.

Kass, J., Jacob, T.C., Kim, P., and Kaplan, J.M. (2001). The EGL-3 proprotein convertase regulates mechanosensory responses of Caenorhabditis elegans. J. Neurosci. *21*, 9265–9272.

Lee, R.Y., Sawin, E.R., Chalfie, M., Horvitz, H.R., and Avery, L. (1999). EAT-4, a homolog of a mammalian sodium-dependent inorganic phosphate cotransporter, is necessary for glutamatergic neurotransmission in Caenorhabditis elegans. J. Neurosci. *19*, 159–167.

Maricq, A.V., Peckol, E., Driscoll, M., and Bargmann, C.I. (1995). Mechanosensory signalling in *C. elegans* mediated by the GLR-1 glutamate receptor. Nature *378*, 78–81.

Momiyama, A. (2000). Distinct synaptic and extrasynaptic NMDA receptors identified in dorsal horn neurones of the adult rat spinal cord. J. Physiol. *523*, 621–628.

Rongo, C., Whitfield, C.W., Rodal, A., Kim, S.K., and Kaplan, J.M. (1998). LIN-10 is a shared component of the polarized protein localization pathways in neurons and epithelia. Cell *94*, 751–759.

Silva, A.P., Carvalho, A.P., Carvalho, C.M., and Malva, J.O. (2001). Modulation of intracellular calcium changes and glutamate release by neuropeptide Y1 and Y2 receptors in the rat hippocampus: differential effects in CA1, CA3 and dentate gyrus. J. Neurochem. *79*, 286–296.

Sommer, B., Kohler, M., Sprengel, R., and Seeburg, P. (1991). RNA editing in brain controls a determinant of ion flow in glutamate-gated channels. Cell *67*, 11–19.

Stern-Bach, Y., Russo, S., Neuman, M., and Rosenmund, C. (1998). A point mutation in the glutamate binding site blocks desensitization of AMPA receptors. Neuron *21*, 907–918.

Takamori, S., Rhee, J.S., Rosenmund, C., and Jahn, R. (2000). Identification of a vesicular glutamate transporter that defines a glutamatergic phenotype in neurons. Nature *407*, 189–194.

Watanabe, S., Kusama-Eguchi, K., Kobayashi, H., and Igarashi, K. (1991). Estimation of polyamine binding to macromolecules and ATP in bovine lymphocytes and rat liver. J. Biol. Chem. *266*, 20803–20809.

White, J.G., Southgate, E., Thomson, J.N., and Brenner, S. (1986). The structure of the nervous system of the nematode *Caenorhabditis elegans*. Phil. Trans. Roy. Soc. (Lond.) B *314*, 1–340.

Woolf, C.J., and Salter, M.W. (2000). Neuronal plasticity: increasing the gain in pain. Science *288*, 1765–1769.

Zheng, Y., Brockie, P.J., Mellem, J.E., Madsen, D.M., and Maricq, A.V. (1999). Neuronal control of locomotion in *C. elegans* is modified by a dominant mutation in the GLR-1 ionotropic glutamate receptor. Neuron *24*, 347–361.

Accession Numbers

The GenBank accession number for the *glr-2* cDNA sequence reported in this paper is AY173128.